RESEARCH ARTICLE

WILEY

Cardioprotection of PLGA/gelatine cardiac patches functionalised with adenosine in a large animal model of ischaemia and reperfusion injury: A feasibility study

Caterina Cristallini[1] [ID] | Giuseppe Vaccari[2] | Niccoletta Barbani[3] | Elisa Cibrario Rocchietti[4] |
Rossella Barberis[5] | Mimmo Falzone[5] | Karine Cabiale[5] | Giovanni Perona[6] |
Elena Bellotti[3] | Raffaella Rastaldo[4] | Silvia Pascale[7] | Pasquale Pagliaro[4] |
Claudia Giachino[4] [ID]

[1] Institute for Chemical and Physical Processes, IPCF, CNR, ss Pisa, Pisa, Italy

[2] IRCCS Cardiovascolare Multimedica, Milan, Italy

[3] Department of Civil and Industrial Engineering, University of Pisa, Pisa, Italy

[4] Department of Clinical and Biological Sciences, University of Turin, Turin, Italy

[5] Life and Device S.r.l., Turin, Italy

[6] Department of Veterinary Science, University of Turin, Turin, Italy

[7] Sorin Group Italia s.r.l., Vercelli, Italy

Correspondence
Caterina Cristallini, Institute for Chemical and Physical Processes, IPCF, CNR, ss Pisa, Pisa, Italy.
Email: c.cristallini@diccism.unipi.it

Claudia Giachino, Department of Clinical and Biological Sciences, University of Turin, Orbassano, Turin 10043, Italy.
Email: claudia.giachino@unito.it

Abstract

The protection from ischaemia-reperfusion-associated myocardial infarction worsening remains a big challenge. We produced a bioartificial 3D cardiac patch with cardioinductive properties on stem cells. Its multilayer structure was functionalised with clinically relevant doses of adenosine. We report here the first study on the potential of these cardiac patches in the controlled delivery of adenosine into the in vivo ischaemic-reperfused pig heart. A Fourier transform infrared chemical imaging approach allowed us to perform a characterisation, complementary to the histological and biochemical analyses on myocardial samples after in vivo patch implantation, increasing the number of investigations and results on the restricted number of pigs (n = 4) employed in this feasibility step. In vitro tests suggested that adenosine was completely released by a functionalised patch, a data that was confirmed in vivo after 24 hr from patch implantation. Moreover, the adenosine-loaded patch enabled a targeted delivery of the drug to the ischaemic-reperfused area of the heart, as highlighted by the activation of the pro-survival signalling reperfusion injury salvage kinases pathway. At 3 months, though limited to one animal, the used methods provided a picture of a tissue in dynamic conditions, associated to the biosynthesis of new collagen and to a non-fibrotic outcome of the healing process underway. The synergistic effect between the functionalised 3D cardiac patch and adenosine cardioprotection might represent a promising innovation in the treatment of reperfusion injury. As this is a feasibility study, the clinical implications of our findings will require further in vivo investigation on larger numbers of ischaemic-reperfused pig hearts.

KEYWORDS

adenosine, cardiac patch, cardioprotection, FT-IR spectroscopy, large-animal model, RISK pathway

1 | INTRODUCTION

Ischaemic heart disease is the leading cause of death in the human population (Gaziano, Bitton, Anand, Abrahams-Gessel, & Murphy, 2009) and the protection against ischaemia-reperfusion (I/R) damage and myocardial infarction (MI) remains a challenge (Pagliaro & Penna, 2014; Yellon & Hausenloy, 2007).

Despite decades of impressive improvements in therapies for patients developing MI, the current therapies do not fully restore the functionality of the damaged myocardial tissue. Paradoxically, about 50% of the myocardium damage after MI is a result of the rapid re-oxygenation of the tissues, known as reperfusion injury (Hausenloy & Yellon, 2008). Reperfusion injury therefore remains a major problem in the treatment of MI patients.

Ischaemic postconditioning, consisting in brief repetitive ischaemic episodes during early reperfusion (Galagudza, Kurapeev, Minasian, Valen, & Vaage, 2004; Zhao, 2010), displays infarct-sparing effect, which can also be achieved by administration of cardioprotective drugs at the time of the myocardial reperfusion or just prior to it (Galagudza, Blokhin, Shmonin, & Mischenko, 2008; Pagliaro & Penna, 2014). Among the pharmacological agents used to induce protection are included adenosine, anaesthetics, cyclosporin-A, NO donors, and P2Y12 inhibitors, administered mostly through intracoronary or intra-venous infusion (Hausenloy et al., 2017; Pagliaro, Femminò, Popara, & Penna, 2018). This pharmacological postconditioning focuses on attenuating the mitochondrial permeability and on promoting the activity of reperfusion injury salvage kinases (RISK), including extracellular-regulated kinase (ERK) and the serine/threonine kinase Akt (Yellon & Hausenloy, 2007).

However, the postconditioning translation into clinical practice has so far been disappointing. Moreover, the pharmacological agents suggested for infarct size limitation have serious side effects when used at cardioprotective doses, which further hinders their clinical use (Pagliaro & Penna, 2014; Sanada, Komuro, & Kitakaze, 2011). One solution to the problem might be a timely and direct delivery of the cardioprotective drugs into ischaemic-reperfused myocardium, in order to administer the drugs in a sufficient concentration to achieve the highest efficiency and limit the side effects (Ye & Yang, 2009).

There is now considerable evidence for adenosine involvement in the mechanisms of cardiac protection from conditioning-induced ischaemia. In particular, by using adenosine and selective agonists and antagonists of several adenosine receptors (Donato et al., 2007; Norton, Jackson, Turner, Virmani, & Forman, 1992; Xi et al., 2009), as well as genetic approaches (Morrison, Tan, Ledent, Mustafa, & Hofmann, 2007; Xi et al., 2008), it has been clearly demonstrated that adenosine and adenosine receptors activation plays a role of para-mount importance in cardioprotection against ischaemia/reperfusion myocardial injury. The current thought is that all the adenosine receptors are needed and interact to produce cardioprotection (Lasley, Kristo, Keith, & Mentzer, 2007; Urmaliya, Pouton, Ledent, Short, & White, 2010; Zhan, McIntosh, & Lasley, 2011). This point of view strongly supports the use of adenosine instead of a specific single receptor agonist.

However, the clinical use of adenosine for myocardial protection has yielded conflicting results and may be limited because of its heavy side effects, such as hypotension and bradycardia (Marzilli, Orsini, Maraccini, & Testa, 2000). It is therefore likely that the modality of drug delivery may be crucial.

We recently produced bioartificial cardiac patches and demonstrated their micropatterning-mediated effect to guide and control proliferation and differentiation of stem cells in cardiac sense (Cristallini et al., 2014; Cristallini et al., 2016).

In this research, we investigated on a small number of pigs (n = 4) the potentiality of multilayered Poly(lactic-co-glycolic acid) (PLGA)/gelatine cardiac patches for the targeted delivery of adenosine into the ischaemic-reperfused large-mammalian heart. The primary goal of this feasibility study was to compare the differences between functionalised and nonfunctionalised patch. Although the exact cardioprotective mechanisms of adenosine are not yet fully understood, we studied the effects of adenosine on some protective/prosurvival kinases (Ovize et al., 2010). The physico-chemical, degradative, and pharmacological characterisation of the scaffolds was performed before and after implantation. Furthermore, histomorphologic, biochemical, and spectroscopic analyses of the explants were carried out, to verify the cardioprotective effect of the adenosine-loaded patch.

2 | MATERIALS AND METHODS

2.1 | Adenosine delivery microstructured multilayer patch (ADMMP) preparation

Our delivery cardiac patch involved the functionalisation with adenosine of a microstructured bilayer based on PLGA (50:50, 40–75 kDa, Sigma Aldrich, USA) and gelatine from porcine skin (gelatine A, Sigma Aldrich, USA), prepared as already described (Cristallini et al., 2016; Khademhosseini et al., 2007; Kim et al., 2012; Zong et al., 2005). The functionalisation method with adenosine (>99%, Sigma Aldrich, USA) was optimised (Figure 1a) in order to reach an immediate and quantitatively elevated release of adenosine in a very short time, as described in Supporting Information. Identical patches, but without adenosine functionalisation, were also produced (MMP). The patches were dried and sterilised according to a previously optimised method (Rosellini, Cristallini, Barbani, Vozzi, & Giusti, 2009).

2.2 | Experimental plan and surgical procedures

Four Large White × Landrace pigs (weight: 46 kg, aged 5 months, sex: female) were utilised. The animals were treated in accordance with the provisions of January 27th, 1992 No 116 Leg. Dec., implementation of Dir No. 86/609/EEC on the protection of animals used
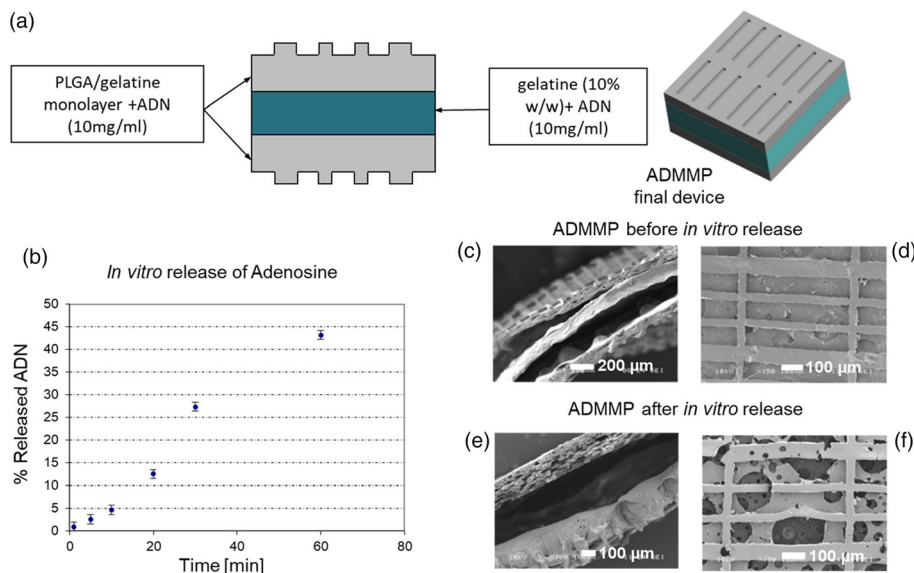
FIGURE 1 (a) Scheme of ADMMP preparation; (b) release trend of adenosine from the sterilised final scaffold with adenosine loading (ADMMP). SEM images of section and surface of ADMMP (c, d) before and (e, f) after release at 24 hr. The section image of ADMMP before release test shows the thickness of the two microstructured external layers and the thickness of the internal layer containing gelatin and adenosine. The section image after 24-hr release in MilliQ water points out an intermediate empty space. The surface image of the scaffold shows the presence of free voids, due to the dissolution of the gelatin and adenosine globular structures [Colour figure can be viewed at wileyonlinelibrary.com]

for experimental and other scientific purposes, art. 5 (a, b, c, d, e), and Leg. Dec. N. 66, published in "Gazzetta Ufficiale della Repubblica Italiana," issue No 61, March 14th, 2014. In line with the EU Directive 2010/63/EU, the principle of the three Rs were implemented in this work. Three animals were sacrificed after 24 hr from intervention (1-3_AMI) and one after 3 months of follow-up (4_AMI) (Table 1).

1_AMI was used to set up the surgical technique, to test the proper number of biopsy samples, and to verify the presence of ischaemic areas after left anterior descending (LAD) coronary artery ligature. To assess the feasibility of patch application on a beating heart and the effect of adenosine on the acute myocardial infarct model, two pigs were sacrificed at 24 hr after implantation of the patches, one

TABLE 1 Experimental plan for the in vivo characterisation of the patch and myocardial tissue

Large Animals White × Landrance Pigs (n = 4)			Patch characterisation after explant	Cardiac tissue characterisation		
	Follow-up	Treatment		Biopsies for biochemical analysis (ischaemic and remote area)	Heart sections Histological analysis	Myocardial sample FTIR, HPLC analysis
1_AMI	24 hr	No patch		10′ before LAD, 45′ after LAD, 10′ LAD reopening, 60′ LAD reopening	Ischaemic area Remote area	
2_AMI + MMP	24 hr	Patch without adenosine	HPLC, FTIR, SEM	10′ before LAD, 45′ after LAD, 10′ LAD reopening, 60′ LAD reopening	Ischaemic area Remote area	Ischaemic area (proximal and distal sections) Remote area
3_AMI + ADMMP	24 hr	Patch with adenosine	HPLC, FTIR, SEM	10′ before LAD, 45′ after LAD, 10′ LAD reopening, 60′ LAD reopening	Ischaemic area Remote area	Ischaemic area (proximal and distal sections) Remote area
4_CMI + ADMMP	3 months	Patch with adenosine		10′ before LAD, 45′ after LAD, 10′ LAD reopening, 60′ LAD reopening	Ischaemic area Remote area	Ischaemic area (proximal and distal sections) Remote area

Note. 1_AMI: animal subjected to LAD to induce ischaemia, follow up at 24-hr acute myocardial infarct model; MMP: multilayer microstructured patch (patch nonloaded with adenosine); ADMMP: adenosine delivery multilayer microstructured patch (patch loaded with adenosine); 2_AMI + MMP: animal subjected to LAD to induce ischaemia, follow up at 24 hr acute myocardial infarct model treated with patch nonloaded with adenosine (MMP); 3_AMI + ADMMP: animal subjected to LAD to induce ischaemia, follow up at 24 hr acute myocardial infarct model treated with patch loaded with adenosine (ADMMP); 4_CMI + ADMMP: animal subjected to LAD to induce ischaemia, follow up at 3 months chronic myocardial infarct model treated with patch loaded with adenosine (ADMMP).

unloaded (2_AMI + MMP) and one loaded with adenosine (3_AMI + ADMMP). To evaluate patch bioabsorbance and preliminary patch effect at a medium follow-up, one pig was sacrificed at 3 months after the implantation of an adenosine-loaded patch (4_AMI + ADMMP). Details concerning surgical procedures and bioptic sampling can be found in Supporting Information. In short, a biopsy was performed 10 min before the LAD occlusion in the area in which ischaemia would have later been induced. For all biopsies, 14G disposable guillotine needles were used. The LAD occlusion was performed by interrupting the anterior descending coronary blood flow with a tourniquet. Five minutes after the LAD ligature, the patch was sutured on the ischaemic area of the myocardium and fixed with four stitches of 5.0 prolene. Two biopsies, one in the ischaemic area and one in a remote area, were performed 45 min after LAD occlusion. After 50 min from the occlusion, the tourniquet was released (LAD reopening, reperfusion step), and 10 min later, two myocardial biopsies, one in the ischaemic area and one in a remote area, were performed. Finally, two additional biopsies, one in the ischaemic area and one in a remote area, were performed 60 min after LAD reopening; the surgical cut was then sutured, and the animal was awakened. The animals were followed daily to measure sensitive parameters such as sensorium, conjunctival mucous membranes, body temperature, ventilation rhythm and breathing rate, and heart rate. Daily dressing of surgical wounds was performed. In the early days of follow-up, the animal was kept under drug therapy that included the use of morphine, analgesics (FANS), and antibiotics.

2.3 | Histomorphological analysis

After the animal sacrifice, the heart was explanted and analysed from a macroscopic and microscopic point of view. The heart was observed, and pictures were taken using a stereoscopic microscope (Leica Z6 APO) to highlight the presence of macroscopic interactions between the patch and the myocardium. At the end of the macroscopic examination, a sample of the myocardium underlying the patch was taken for histological analysis, and a sample of the myocardium in an area not interested by the ischaemic event was taken as a control. The obtained samples were processed for paraffin embedding. The samples were sliced in 4- to 5-μm serial sections and stained with haematoxylin/eosin (HE) and Gomori stains. The slides were observed and photographed under a biological microscope (Nikon Eclipse E600). Ten pictures per animal, at 40× magnification, were obtained from the HE-stained serial sections. The pictures were taken randomly in the area immediately under the patch. The epicardial thickness was measured using the image analysis software Image-Pro Premier 9.1 (Media Cybernetics). Ten linear measures were performed on each sample (2_AMI + MMP, 3_AMI + ADMMP, and 4_AMI + ADMMP) and the epicardial thickness calculated as the mean of the obtained values. Inflammatory cells (macrophages, eosinophils, neutrophils, lymphocytes, and mastocytes) were distinguished based on their morphology and dye affinities. The total cell number

and the inflammatory cell number were accurately counted using the Image-Pro Premier 9.1 software. Other samples, both underlying the patch and in a remote area, were taken and frozen for physico-chemical analyses.

2.4 | Biochemical study of the biopsies by means of western blot analysis

Western blot was used to analyse the heart biopsies. Specific antibodies against porcine total AKT (diluted 1:1000), phosphorylated Akt (diluted 1:1000), total ERK 1/2 (diluted 1:1000), phosphorylated ERK 1/2 (Diluted 1:500; all from Cell Signaling Technology, USA), and α-actinin (1:10000, Sigma-Aldrich, USA) were used. Expression levels of phospho-AKT and phospho-ERK 1/2 were normalised to both α-actinin and total AKT/total ERK proteins. For each animal, the expression levels of phospho-AKT and phospho-ERK proteins detected in the biopsies, sampled after either LAD ligature or LAD reopening, were normalised against the expression levels detected in the biopsies taken before LAD ligature, to reduce intertest animal biological differences.

2.5 | In vitro morphological, physico-chemical, and functional ADMMP characterisation before and after apposition onto myocardium

Release tests of adenosine from ADMMP were performed by high-performance liquid chromatography (HPLC, Perkin Elmer Series 200) as described in Supporting Information. Morphological analyses were carried out on gold sputtered samples by scanning electron microscopy (SEM, Jeol JSM 5600). All the samples were lyophilised before analysis. The chemical analysis was carried out by Fourier transform infrared (FT-IR) spectroscopy chemical imaging (Perkin Elmer Spotlight 300). FTIR spectroscopy is well known as a sensitive tool in identifying chemical structures of organic compounds, including synthetic and biological polymers. In this study, FTIR technique was used to evaluate both the chemical composition of patch and possible alterations of protein conformation and nucleic acids in the treated myocardial tissue.

The attenuated total reflectance (ATR) sampling technique was performed on small fragments of ADMMP or on myocardial samples. Spectral images were acquired in μATR mode (the spectral resolution was 4 cm^{-1}, and the spatial resolution was 100 × 100 μm). The spectra were collected by putting in contact the ATR objective and the sample and collecting the spectrum generated from the surface layer of the sample. The obtained correlation map indicates the areas of each image where the spectra are most similar to a reference spectrum. The band ratio analysis involves the measurement of the band intensity or area of an internal reference, with respect to that of a band of interest.

FT-IR analysis was carried out directly on the patch detached from 2_AMI + ADMMP and 3_AMI + ADMMP tissues after 24 hr of follow-up. The analysis was not feasible on the patch from the 4_AMI + ADMMP tissue, because the patch was completely reabsorbed after 3 months. A FT-IR analysis was carried out on

myocardium samples both from the ischaemic area and remote areas after 24 hr and 90 days of follow-up. The myocardium samples underlying the patch were further sliced, obtaining closer (proximal) and deeper (distal) sections respect to patch positioning. Before FT-IR analysis, all samples were lyophilised at the same temperature rate.

FT-IR chemical imaging allows to gain information about the chemical composition of healthy and diseased human tissues (Liu et al., 1996; Liu, Dixon, & Mantsch, 1999); the most important parameters to distinguish acute and chronic MI are reported in Table 2.

3 | RESULTS

3.1 | In vitro characterisation of ADMMP before implantation

After sterilisation, ADMMP was subjected to the in vitro release test showing a high delivery in the interval from 1 min to 1 hr (Figure 1 b), corresponding to 43% with respect to the amount contained in the device (17.6 ± 0.2 mg), in line with the doses of intraluminally administered adenosine (Ross et al., 2005).

SEM images of ADMMP before and after adenosine release (Figure 1c–f) and spectra obtained by FT-IR chemical imaging confirmed that the adenosine was completely released as described in Supporting Information.

3.2 | Histomorphological analyses

The hearts were explanted at either 24 hr or 3 months follow-up. The explanted hearts were observed as intact (2_AMI + MMP, 3_AMI + ADMMP, and 4_AMI + ADMMP) or after accurate slicing (1_AMI) by stereomicroscopy, to highlight possible alterations and/or interactions between patch and cardiac tissue. No important macroscopic alterations were evidenced in the examined hearts; only some areas of pericardial–epicardial adhesion, due to implant procedures, was visible in all the explants. A well-localised necrotic area was visible in 1_AMI after LAD ligature; histology showed blood vessels necrosis, vacuolisation, inflammatory cells infiltration, and degenerated red blood cells (Figure 2a).

The patches appeared well adherent to the epicardial surface in both 2_AMI + MMP and 3_AMI + ADMMP (24-hr follow-up); the patch in 4_AMI + ADMMP, however, at 3-month follow-up, appeared completely reabsorbed with only the stitches remaining visible (Figure 2m). No tissue growth due to foreign body reaction was detectable in any of the hearts.

The histological examination corroborated the macroscopic data. Some thrombus depositions were visible on the outer surface of 2_AMI + MMP. A good adhesion of the patch to the underlying myocardium was confirmed in the samples at 24-hr follow-up (Figure 2b). A complete absorption of the patch in 4_AMI + ADMMP was also histologically confirmed (Figure 2n). Further, the histological analysis showed a moderate epicardial thickening; after morphometrical analysis, it resulted in 0.692 ± .023 mm in the 24-hr follow-up samples and in 0.797 ± 0.031 mm in the 3-month follow-up samples; as the two data can be considered comparable, the epicardial thickening could be ascribed to pericardium–epicardium adhesion.

Inflammatory cells were present in all the samples, though in variable numbers: In 2_AMI + MMP, abundant inflammatory cells were present under the epicardial surface and inside the myocardium (Figure 2c–f); in 3_AMI + ADMMP and in 4_AMI + ADMMP, inflammatory cells were less abundant and localised only under the epicardial layer (Figure 2i,j). This suggested a lower inflammation in the animals in which the patch with adenosine (ADMMP) was implanted.

The histological analysis carried out on 4_AMI + ADMMP showed the presence of unaltered cardiomyocytes together with areas of myxoid tissue (Figure 2o,p). Although, in the 2_AMI + MMP samples, large areas of heavily degenerated myocardial tissue with disarranged myofibrillar structure of cardiomyocytes (Gomori-stain; Figure 2g, h) were visible, in 3_AMI + ADMMP, only limited areas of suffering, yet not degenerated, myocardial tissue with preserved myofibrillar structure of cardiomyocytes (Gomori stain) were present (Figure 2k,l).

Histomorphometrical analysis showed that the total cell number was considerably higher in 2_AMI + MMP than 3_AMI + ADMMP, and the number of inflammatory cells was, respectively, 62% and 38% of the total number. Furthermore, in 2_AMI + MMP, mononucleates seemed to outnumber polymorphonucleates, whereas in 3_AMI + ADMMP, most of the inflammatory cells were polymorphonucleates, mostly eosinophils. All these findings suggested protective effects of adenosine-loaded patches.

TABLE 2 FT-IR parameters in acute and chronic myocardial infarction (MI)

Acute MI		Chronic MI	
Parameters	Tissue correlation	Parameters	Tissue correlation
Variations of the peak of GAG/protein ratio	Early tissue modification in infarcted regions	Increase of the band intensity at 1,082 cm^{-1} and at 1,662 cm^{-1} in the region of 31-helix of collagen	Collagen deposition
Reduction of C=O stretching vibrations of: phospholipids (1,738 cm^{-1}) nucleic acids (1,721 cm^{-1})	Loss of cellular components of the cardiac tissue (myocytes, quiescent fibroblasts)	Variation of the CH$_2$/CH$_3$ peak ratio CH$_2$ at 2,852–2,926 cm^{-1} CH$_3$ at 2,956 cm^{-1}	Reduction of the lipid content respect to collagen fibrotic tissue
Modification of protein secondary structure	Modification of ECM proteins	Increase of absorption at 1,638 cm^{-1} in a spectral region of collagen I triple helix	Fibrotic tissue
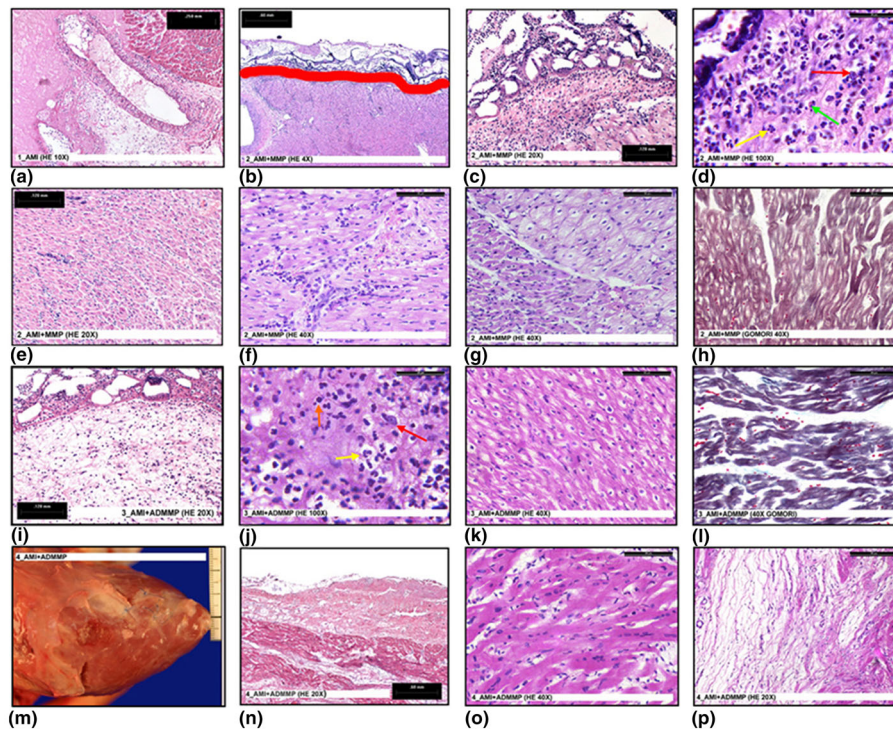
FIGURE 2 (a) A necrotic myocardium area in 1_AMI (HE 10×); (b) patch adhesion in 2_AMI + MMP. Red line shows the border between patch (up) and epicardium (down) (HE 4×); (c) abundant inflammatory cells under the epicardial layer in 2_AMI + MMP (HE 20×); (d) abundant inflammatory cells under the epicardial layer in 2_AMI + MMP. High magnification (HE 100×). The image shows the presence of macrophages (red arrow) neutrophils (yellow arrow) and eosinophils (green arrow); (e) inflammatory cells inside the myocardium in 2_AMI + MMP (HE 20×); (f) inflammatory cells inside the myocardium in 2_AMI + MMP. High magnification (HE 40×); (g) normal (on the left) and degenerated (on the right) myocardium tissue in 2_AMI + MMP (HE 40×); (h) degenerated myocardium in 2_AMI + MMP (Gomori 40×); (i) inflammatory cells under the epicardial layer in 3_AMI + ADMMP (HE 20×); (j) inflammatory cells under the epicardial layer in 3_AMI + ADMMP. High magnification (HE 100×). The image shows the presence of macrophages (red arrow), neutrophils (yellow arrow), and lymphocytes (orange arrow); (k) suffering myocardium in 3_AMI + ADMMP (HE 40×); (l) suffering myocardium in 3_AMI + ADMMP (Gomori 40×); (m) macroscopic image of the reabsorbed patch in 4_AMI + ADMMP; (n) microscopic image of the reabsorbed patch in 4_AMI + ADMMP (HE 20×); (o) normal myocardium in 4_AMI + ADMMP (HE 40×); (p) mixoid tissue in 4_AMI + ADMMP (HE 20×) [Colour figure can be viewed at wileyonlinelibrary.com]

3.3 | Biochemical study

To dissect the putative mechanisms of the cardioprotective effects of adenosine-loaded patches, we quantified the RISK pathway activation on the heart biopsies taken at 0–10-60 min time course after LAD. The left ventricular (LV) tissue from the non-infarcted zone (remote area biopsies) showed no change in phospho-ERK and phospho-AKT expression (data not shown). However, if compared with the 2_AMI + MMP animal that did not show any significant signs of activation, LV tissue sampled close to the ischaemic area from 3_AMI + ADMMP and 4_AMI + ADMMP showed RISK pathway activation. An increase in AKT phosphorylation was highlighted in 3_AMI + ADMMP, even in the biopsy taken before LAD reopening (time: 0 min, about 45 min from scaffold implantation; Figure 3a,c). However, phospho-AKT was not pointed out in the biopsies sampled after LAD reopening in this condition. 4_AMI + ADMMP showed an increase in ERK 1/2 phosphorylation in the biopsy taken before LAD reopening, with a further increase in the biopsy taken 10 min after LAD reopening (time: 10 min, Figure 3b,d). In both animals,

the activation of the RISK pathway turned back to basal levels after 60 min from LAD reopening, as expected (time: 60 min, Figure 3).

These findings suggest that ADMMP implant before reperfusion activates signalling pathways that protect against reperfusion injury during MI.

3.4 | Physico-chemical, degradative, and pharmacological characterisation of the scaffolds after explant

The results obtained by HPLC and FT-IR on the patch at 24 hr of follow-up revealed no appreciable amounts of adenosine in agreement with in vitro tests. The in vitro analysis carried out directly on the tissue underlying the patch after 24 hr showed the presence of not yet metabolised adenosine corresponding to 13% w/w, compared with that initially present in the scaffold. The SEM analysis of the patch explanted at 24 hr shows a surface with the micropatterning lines only slightly modified (Supporting Information). In addition, in accordance with histological results, FT-IR analysis confirmed a good adhesion of the scaffold to the tissue as evidenced by the presence
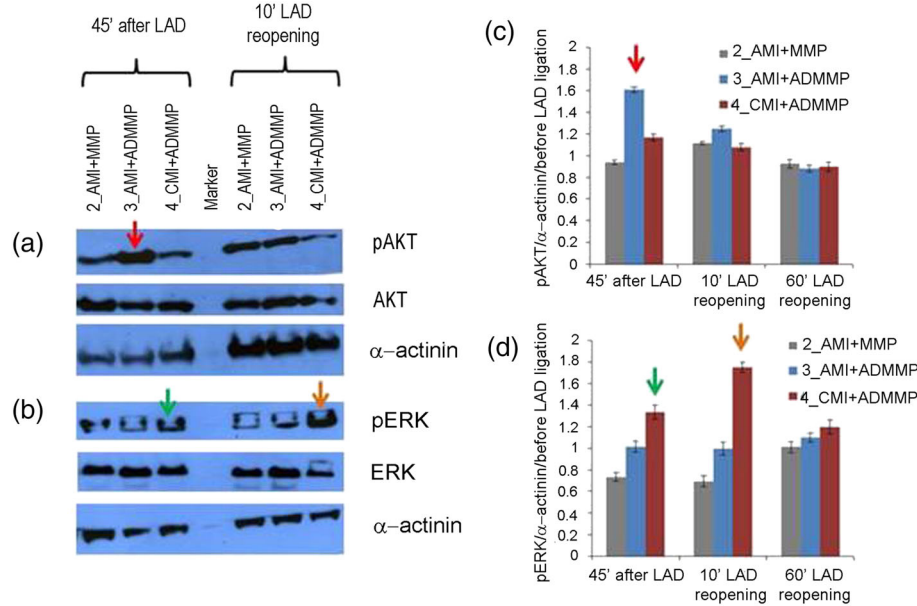
FIGURE 3 Analysis of reperfusion injury salvage kinase (RISK) pathway activation: (a, b) western blot analysis of phosphorylated extracellular signal-regulated kinase AKT (pAKT) and phosphorylated ERK 1/2 (pERK 1/2) normalised to total AKT and ERK 1/2 proteins and to α-actinin; one representative experiment (out of three) per animal is shown; (c, d) quantification of western blots for pAKT and pERK normalised to α-actinin and to phosphorylated proteins, detected in the biopsies taken before LAD ligature. SEM of three independent blot quantifications per animal is shown. Differences exceeding ±3 *SEM* were considered significant and indicated by coloured arrows. A red arrow indicates AKT phosphorylation increase after LAD ligature in animal 3_AMI + ADMMP versus 2_AMI + MMP (1.61 vs. 0.94), a green arrow indicates ERK 1/2 phosphorylation increase after LAD ligature in animal 4_AMI + ADMMP versus 2_AMI + MMP (1.33 versus 0.73), and an orange arrow indicates ERK 1/2 phosphorylation increase 10 min after LAD reopening in animal 4_AMI + ADMMP versus 2_AMI + MMP (1.75 versus 0.69) [Colour figure can be viewed at wileyonlinelibrary.com]
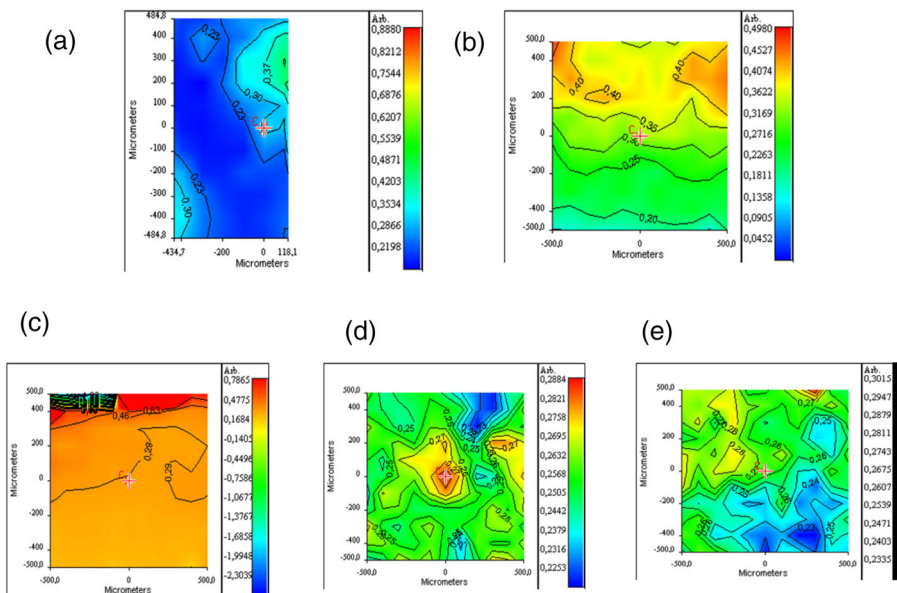
FIGURE 4 FT-IR chemical imaging: (a) GAG/protein ratio at the interface with ADMMP in myocardial samples of 3_AMI + ADMMP, (b) GAG/protein ratio in myocardial samples of 2_AMI + MMP. GAG/protein ratio for (c) control healthy tissue, (d) myocardial tissue of 4_AMI + ADMMP in the correspondence of the proximal area, and (e) distal area respect to ADMMP position [Colour figure can be viewed at wileyonlinelibrary.com]

of typical peaks of the polymeric materials (i.e., ester C=O stretching at 1,740 cm^{-1}) at the level of the interface with the tissue (Supporting Information).

After 3 months of follow-up, HPLC did not detect the presence of adenosine where ADMMP was implanted and revealed that the patch was completely degraded. FT-IR analyses confirmed the absence of scaffold components, indicating a complete resorption of the material (Supporting Information).

3.5 | Physico-chemical analysis on myocardial tissue by means of FT-IR chemical imaging

The GAG/protein ratio at the interface with the patch was evaluated in the myocardial samples of 2_AMI + MMP and 3_AMI + ADMMP and compared with the GAG/protein ratio in a remote area of the same animal (control; Figure 4a,b). No substantial differences were found between the GAG/protein ratio for myocardial

3_AMI + ADMMP samples taken at the level of the proximal (R = 0.23–0.30) and distal section (R = 0.24-0.33). These results are in line with the value obtained from a control area (R = 0.29). As to 2_AMI + MMP myocardial tissue, a significant variability of the GAG/protein ratio (R = 0.18–0.44), indicative of GAG component degradation (low values) and interstitial oedema (high values), can be observed. In Figure 4c–e, the chemical maps of tissues sampled at proximal and distal level are reported and compared with that of the control tissue. The mean values measured for the proximal area (R = 0.23–0.28) and for the distal area (R = 0.23–0.28) are only in limited domains slightly lower than the one measured for healthy tissue (R = 0.29). This reduction is likely not due to a fibrosis condition (a process that can last 12 months after the injury) but to the presence of collagen deposition areas, an event that is part of the normal wound healing process.

For 4_AMI + ADMMP tissue, CH$_2$/CH$_3$ stretching peak ratio, GAG/protein ratio, and amide deconvolution were the considered parameters. The cellularisation of the tissue was evaluated by CH$_2$/
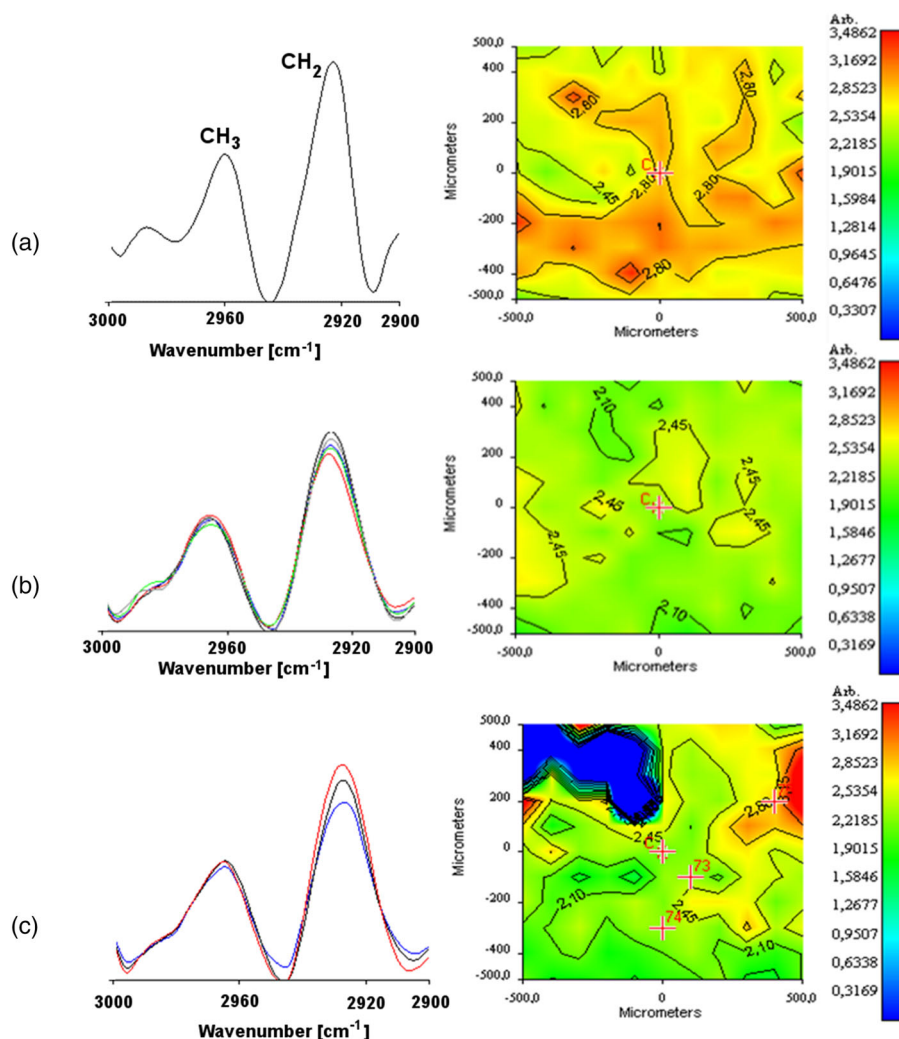
FIGURE 5 FT-IR chemical imaging spectra, second derivative spectra, and corresponding chemical map: (a) CH$_2$/CH$_3$ stretching peak ratio for control healthy tissue, (b) for myocardial samples of 4_AMI + ADMMP in the correspondence of proximal area, and (c) distal area respect to ADMMP position [Colour figure can be viewed at wileyonlinelibrary.com]
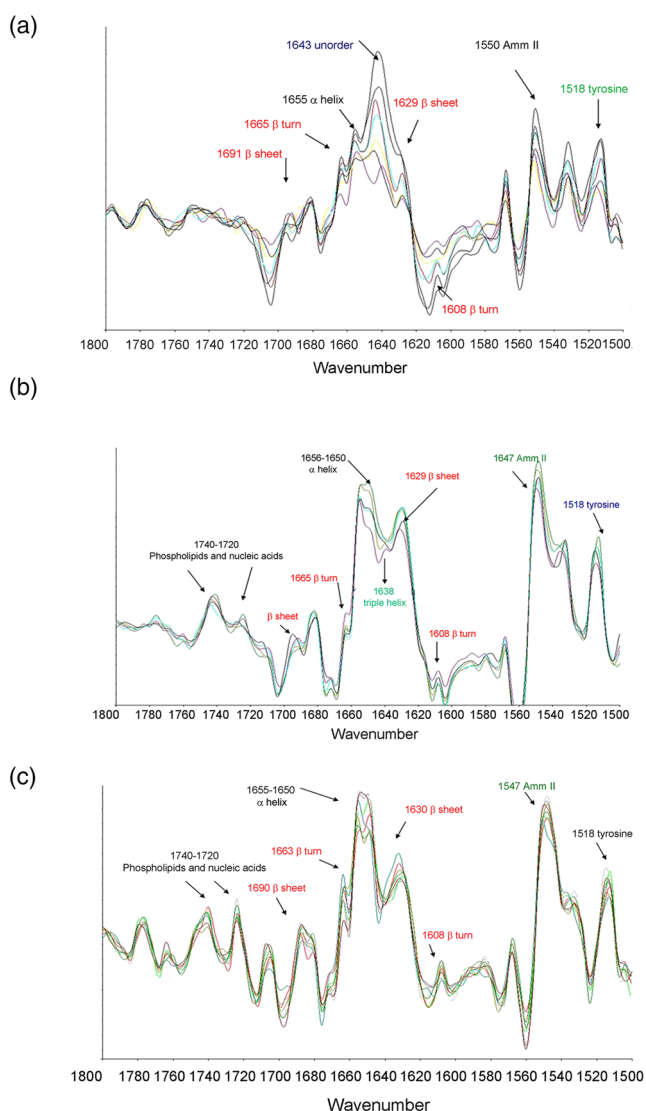
CH$_3$ stretching peak ratio also for 4_AMI + ADMMP. In Figure 5, second derivative spectra and corresponding chemical maps for a healthy tissue and for the myocardial tissue of 4_AMI + ADMMP acquired at both proximal and distal levels are reported. It is important to state that the CH$_3$ stretching band can be attributed to the presence of membrane phospholipids, whereas the CH$_2$ stretching peak derived from glycine and proline residues of collagen. The CH$_2$/CH$_3$ (2,926 cm^{-1}/2,956 cm^{-1}) peak ratio can therefore be considered as indicative of both cellularisation and collagen deposition. As evidenced by the comparison of ratio values corresponding to R = 2.45–2.80 for an healthy tissue, R = 2.10–2.45 for tissue at proximal level, and R = 2.10–2.80 for the tissue at distal level, no substantial variations in the ratio are observed with respect to the control tissue, indicating that there is no significant decrease of cells

and/or increase of collagen in the tissue that was in contact with the device after 3 months.

In Figure 6, the second derivative spectra are reported, acquired from the maps of tissue after 3 months of contact with the ADMMP at proximal level and compared with those acquired from a negative control (healthy myocardial tissue) and from a positive control (infarcted tissue). In the spectrum of negative control (Figure 6a), typical peaks of a healthy tissue can be observed. In Figure 6b, the second derivative spectrum from a region involved in an infarction process was reported. Substantial differences are evident respect to the spectrum from healthy tissue; in particular, it can be observed a reduction of intensity of the bands at 1,740–1,720 cm^{-1}, reflecting phagocytosis of membrane lipids and nucleic acid after infarction. In addition, an intense absorption of the amide I at 1,643 cm^{-1}, typical of the infarcted tissue, was revealed. Furthermore, the adsorption at 1,655 cm^{-1} and at 1,629 cm^{-1} due to α-helical and β-turn protein structure, respectively, is reduced in infarcted heart tissue.

In Figure 6c, the spectrum of the proximal area at the interface with the functionalized patch was reported. The main absorption of amide I at 1,643 cm^{-1} that appears in the infarcted tissue is not significant in the area in contact with the device. In addition, the band at 1,650 cm^{-1} is more intense than that at 1,655 cm^{-1}, suggesting a deposition of newly synthesised collagen. Particularly, significant is the absence, in the proximal area, of the band absorption at 1,638 cm^{-1}, relative to the triple helical structure of collagen in fibrotic conditions. The presence of bands in the 1,740 to 1,720-cm^{-1} range is highly significant for a good re-cellularisation of post-infarction tissue.

4 | DISCUSSION

The present work represents a feasibility study for the employment of an innovative PLGA/gelatine cardiac patch functionalised wth adenosine for cardioprotective purposes in a large-animal model.

On the basis of our previous encouraging results with microstructured (Cristallini et al., 2014) and multilayer (Cristallini et al., 2016) patches for stem cell differentiation, the present study was designed to expand our knowledge on a functionalized PLGA/gelatine cardiac patch as drug carrier in a large-animal model in order to validate the novel paradigm of *controlled adenosine delivery* to reduce myocardial reperfusion injury, using a patch able also to guide the cardiac tissue regeneration.

Physico-chemical and morphological analyses confirmed the validity of the used loading method, showing how the assembling of the scaffold represents an optimal platform for a quick and sustained release of the cardio-protective agent. After completion of the drug reservoir function, reducing the reperfusion injury, the patch can continue to carry out its second function, which consists in driving the regenerative processes, as already described in our previous work (Cristallini et al., 2014; Cristallini et al., 2016).

In vitro and in vivo tests indicate that the amount of adenosine in the intermediate layer is completely released. In particular, in vivo, at

FIGURE 6 Second derivative spectra acquired from (a) the control of healthy tissue sections, (b) infarcted area not treated with ADMMP, and (c) proximal area at the interface with ADMMP in 4_AMI + ADMMP [Colour figure can be viewed at wileyonlinelibrary.com]

24 hr of follow-up, adenosine was completely released from the patch, whereas part of the drug was still present in the tissue underneath the patch and not yet metabolised. Remarkably, the dose of adenosine that we used, about 11 mg within the myocardial area at risk (corresponding to about 20 g of myocardium), was concentrated and present in the tissue for a long time. This dose therefore represents several times the usual dose (10–12 mg/kg for the entire body) intravenously infused for 3 hours (Ross et al., 2005).

A series of advantages for our delivery system can therefore be considered as compared with direct injection: (a) It allows an early application of adenosine, which will be present at the moment of reperfusion when the cardioprotective mechanisms must be already operative; (b) it does not require a transit in the blood, where the half-life of adenosine is very short; (c) it allows to achieve higher intramyocardial concentrations in a brief period of time and for long periods when compared with the intravenous infusion, thus limiting local and systemic adverse effects (eg, it limits the possibility that adenosine reaches the atrial/nodal tissue where it can alter impulse genesis/conduction and/or the systemic arterioles thus inducing hypotension); (d) finally, our system allows adenosine application to the myocardial tissue even in the absence or limited coronary flow, and under these circumstances of no-reflow phenomenon, its biological effects could also last much longer than expected.

The biochemical findings suggest that adenosine released from ADMMP promotes transient RISK pathway activity, including phospho-ERK and phospho-AKT. Several studies have suggested that an increasing number of agents including adenosine, adipocytokines, erythropoietin, insulin, natriuretic peptides, and statins, to name a few, may reduce ischaemia/reperfusion injury via the RISK pathway activation when administered at the beginning of cardiac reperfusion. However, the transition to the clinical arena has been fairly successful. Nevertheless, and despite the controversial results with adenosine, this endogenous factor resulted superior to other drugs in inducing cardioprotection in several clinical studies (Niccoli et al., 2013; Singh et al., 2012). Here, the promising protective effect of very high doses of adenosine, with no evidences of side effects, is corroborated by the improvement of other signs and features of the lesion and by the well-being of the treated animals.

It has been recently demonstrated that the microscopic morphology and the chemical composition of the tissue are particularly relevant for MI progression (Colley, Kazarian, Weinberg, & Lever, 2004; Yang et al., 2011). In this work, the use of FT-IR allowed to gather specific chemical information on different components within an MI site, discriminating between altered and healthy regions and pointing out the effects of a patch both loaded with adenosine (ADMMP) and not loaded (MMP) on the infarcted areas. One important advantage is the possibility to carry out the analysis without the need of staining the area of interest, allowing obtaining information about molecular composition on heterogeneous substrates, such as biological samples (Yang et al., 2011). Altogether, this and other studies (Gough, Zelinski, Wiens, Rak, & Dixon, 2003; Liu et al., 1996; Liu et al., 1999; Samouillan et al., 2017) confirm that FT-IR chemical analysis can be used to evaluate pathological changes in MI in a very short time, and the results are consistent with the infarction fibrosis region shown with HE staining. The possibility to complement histological and biochemical analyses with the FT-IR chemical imaging technique increases the number of investigations while limiting the number of animals to be employed; this is very important as it impinges upon the highly desirable accomplishment of the 3Rs (reduce, refine, and replace) rule in bio-nanomedicine applications (Accomasso, Cristallini, & Giachino, 2018).

The histological, histomorphometrical, and FT-IR analyses carried out at the level of the tissue/patch interface provided a picture of a tissue in dynamic conditions, in which normal cardiomyocytes are associated to the biosynthesis of new collagen and to a less-fibrotic outcome of the healing process in hearts treated with functionalised patches.

Due to the low number of analysed samples, this represents a feasibility study for an innovative and unconventional approach to cardiovascular disease, and the clinical implications of these findings will require further investigation. Concerning the pharmacological aspect, several groups of drugs with different mechanisms of action might potentially be targeted to the heart using PLGA/gelatine cardiac patches (e.g., bradykinin, opioids, insulin-like growth factor-1, transforming growth factor-β1, cyclosporine A, and nicorandil). Indeed, a widespread clinical use of these drugs at the required doses for a cardioprotective response was hampered by the high risk of dangerous side effects. The targeted delivery strategy proposed here may help to overcome these limitations.

In conclusion, a PLGA/gelatine 3D cardiac patch was functionalised with adenosine in order to obtain a synergistic effect between patch cardio-inductivity and adenosine cardioprotection, a previously unexplored combination at the basis of a recent international patent (PCT/IB2014/0580025). The major finding is that the functionalisation of bilayered PLGA/gelatine cardiac patches with adenosine enables its targeted delivery to the ischaemic-reperfused area of the heart, where it promotes several beneficial effects. Besides the activation of pro-survival signalling pathways, the patch functionalised with adenosine apparently promotes a more pronounced cellularisation at 24 hr follow-up and a non-fibrotic outcome at 3 months follow-up.

CONFLICT OF INTEREST

The authors declare no conflicts of interest.

AUTHOR CONTRIBUTION

C. Cristallini and C. Giachino is responsible for the conception and design, analysis, and interpretation of data and paper drafting; G.

ORCID

Caterina Cristallini https://orcid.org/0000-0002-5924-8401
Claudia Giachino https://orcid.org/0000-0001-7957-3925

REFERENCES

Accomasso, L., Cristallini, C., & Giachino, C. (2018). Risk assessment and risk minimization in nanomedicine; a need for predictive, alternative, and 3Rs strategies. *Frontiers in Pharmacology*, *9*, 228. https://doi.org/10.3389/fphar.2018.00228

Colley, C. S., Kazarian, S. G., Weinberg, P. D., & Lever, M. J. (2004). Spectroscopic imaging of arteries and atherosclerotic plaques. *Biopolymers*, *74*, 328–335. https://doi.org/10.1002/bip.20069

Cristallini, C., Cibrario Rocchietti, E., Accomasso, L., Folino, A., Gallina, C., Muratori, L., ... Giachino, C. (2014). The effect of bioartificial constructs that mimic myocardial structure and biomechanical properties on stem cell commitment towards cardiac lineage. *Biomaterials*, *35*, 92–104. https://doi.org/10.1016/j.biomaterials.2013.09.058

Cristallini, C., Cibrario Rocchietti, E., Gagliardi, M., Mortati, L., Saviozzi, S., Bellotti, E., ... Giachino, C. (2016). Micro and macro-structured PLGA/gelatin scaffolds promote early cardiogenic commitment of human mesenchymal stem cells in vitro. *Stem Cells International*, *2016*:7176154, 1–16. https://doi.org/10.1155/2016/7176154

Donato, M., D'Annunzio, V., Berg, G., Gonzalez, G., Schreier, L., Morales, C., ... Gelpi, R. J. (2007). Ischemic postconditioning reduces infarct size by activation of A1 receptors and K+(ATP) channels in both normal and hypercholesterolemic rabbits. *Journal of Cardiovascular Pharmacology*, *49*, 287–292. https://doi.org/10.1097/FJC.0b013e31803c55fe

Galagudza, M., Blokhin, I., Shmonin, A., & Mischenko, K. (2008). Reduction of myocardial ischemia-reperfusion injury with pre- and postconditioning: Molecular mechanisms and therapeutic targets. *Cardiovascular & Hematological Disorders Drug Targets*, *8*, 47–65. https://doi.org/10.2174/187152908783884966

Galagudza, M., Kurapeev, D., Minasian, S., Valen, G., & Vaage, J. (2004). Ischemic postconditioning: Brief ischemia during reperfusion converts persistent ventricular fibrillation into regular rhythm. *European Journal of Cardio-Thoracic Surgery*, *25*, 1006–1010. https://doi.org/10.1016/j.ejcts.2004.02.003

Gaziano, T. A., Bitton, A., Anand, S., Abrahams-Gessel, S., & Murphy, A. (2009). Growing epidemic coronary heart disease in low- and middle-income countries. *Current Problems in Cardiology*, *35*, 72–115. https://doi.org/10.1016/j.cpcardiol.2009.10.002

Gough, K. M., Zelinski, D., Wiens, R., Rak, M., & Dixon, I. M. C. (2003). Fourier transform infrared evaluation of microscopic scarring in the cardiomyopathic heart: Effect of chronic AT_1 suppression. *Analytical Biochemistry*, *316*, 232–242. https://doi.org/10.1016/S0003-2697(03)00039-3

Hausenloy, D. J., Garcia-Dorado, D., Botker, H. E., Davidson, S. M., Downey, J., Engel, F. B., ... Ferdinandy, P. (2017). Novel targets and future strategies for acute cardioprotection: Position Paper of the European Society of Cardiology Working Group on Cellular Biology of the Heart. *Cardiovascular Research*, *113*, 564–585. https://doi.org/10.1093/cvr/cvx049

Hausenloy, D. J., & Yellon, D. M. (2008). Time to take myocardial reperfusion injury seriously. *The New England Journal of Medicine*, *359*, 518–520. https://doi.org/10.1056/NEJMe0803746

Khademhosseini, A., Eng, G., Yeh, J., Kucharczyk, P. A., Langer, R., Vunjak-Novakovic, G., & Radisic, M. (2007). Microfluidic patterning for fabrication of contractile cardiac organoids. *Biomedical Microdevices*, *9*, 149–157. https://doi.org/10.1007/s10544-006-9013-7

Kim, D. H., Kshitiz, Smith, R. R., Kim, P., Ahn, E. H., Kim, H. N., ... Levchenko, A. (2012). Nanopatterned cardiac cell patches promote stem cell niche formation and myocardial regeneration. *Integrative Biology*, *4*, 1019–1033. https://doi.org/10.1039/c2ib20067h

Lasley, R. D., Kristo, G., Keith, B. J., & Mentzer, R. M. Jr. (2007). The A2A/A2B receptor antagonist ZM-241385 blocks the cardioprotective effect of adenosine agonist pretreatment in in vivo rat myocardium. *American Journal of Physiology. Heart and Circulatory Physiology*, *292*, H426–H431. https://doi.org/10.1152/ajpheart.00675.2006

Liu, K.-Z., Dixon, I. M. C., & Mantsch, H. H. (1999). Distribution of collagen deposition in cardiomyopathic hamster hearts determined by infrared microscopy. *Cardiovascular Pathology*, *8*, 41–47. https://doi.org/10.1016/S1054-8807(98)00024-6

Liu, K.-Z., Jackson, M., Sowa, M. G., Ju, H., Dixon, I. M. C., & Mantsch, H. H. (1996). Modification of the extracellular matrix following myocardial infarction monitored by FTIR spectroscopy. *Biochimica et Biophysica Acta*, *1315*, 73–77. https://doi.org/10.1016/0925-4439(95)00118-2

Marzilli, M., Orsini, E., Maraccini, P., & Testa, R. (2000). Beneficial effects of intracoronary adenosine as an adjunct to primary angioplasty in acute myocardial infarction. *Circulation*, *101*, 2154–2159. https://doi.org/10.1161/01.CIR.101.18.2154

Morrison, R. R., Tan, X. L., Ledent, C., Mustafa, S. J., & Hofmann, P. A. (2007). Targeted deletion of A2A adenosine receptors attenuates the protective effects of myocardial postconditioning. *American Journal of Physiology. Heart and Circulatory Physiology*, *293*, H2523–H2529. https://doi.org/10.1152/ajpheart.00612.2007

Niccoli, G., Rigattieri, S., De Vita, M. R., Valgimigli, M., Corvo, P., Fabbiocchi, F., ... Crea, F. (2013). Open-label, randomized, placebo-controlled evaluation of intracoronary adenosine or nitroprusside after thrombus aspiration during primary percutaneous coronary intervention for the prevention of microvascular obstruction in acute myocardial infarction: the REOPEN-AMI study (Intracoronary Nitroprusside Versus Adenosine in Acute Myocardial Infarction). *JACC. Cardiovascular Interventions*, *6*, 580–589. https://doi.org/10.1016/j.jcin.2013.02.009

Norton, E. D., Jackson, E. K., Turner, M. B., Virmani, R., & Forman, M. B. (1992). The effects of intravenous infusions of selective adenosine A1-receptor and A2-receptor agonists on myocardial reperfusion injury. *American Heart Journal*, *123*, 332–338. https://doi.org/10.1016/0002-8703(92)90643-A

Ovize, M., Baxter, G. F., Di Lisa, F., Ferdinandy, P., Garcia-Dorado, D., Hausenloy, D. J., ... Working Group of Cellular Biology of Heart of European Society of Cardiology (2010). Postconditioning and protection from reperfusion injury: Where do we stand? Position paper from the Working Group of Cellular Biology of the Heart of the European Society of Cardiology. *Cardiovascular Research*, *87*, 406–423. https://doi.org/10.1093/cvr/cvq129

Pagliaro, P., Femminò, S., Popara, J., & Penna, C. (2018). Mitochondria in cardiac postconditioning. *Frontiers in Physiology*, *9*, 287. https://doi.org/10.3389/fphys.2018.00287

Pagliaro, P., & Penna, C. (2014). Redox. Signalling and cardioprotection: Translatability and mechanism. *British Journal of Pharmacology*, *172*, 1974–1995. https://doi.org/10.1111/bph.12975

Rosellini, E., Cristallini, C., Barbani, N., Vozzi, G., & Giusti, P. (2009). Preparation and characterization of alginate/gelatin blend films for cardiac tissue engineering. *Journal of Biomedical Materials Research Part A*, *91A*, 447–453. https://doi.org/10.1002/jbm.a.32216

Ross, A. M., Gibbons, R. J., Stone, G. W., Kloner, R. A., Alexander, R. W., & AMISTAD-II Investigators (2005). A randomized, double-blinded, placebo-controlled multicenter trial of adenosine as an adjunct to reperfusion in the treatment of acute myocardial infarction (AMISTAD-II). *Journal of the American College of Cardiology*, *45*, 1775–1780. https://doi.org/10.1016/j.jacc.2005.02.061

Samouillan, V., Revuelta-López, E., Soler-Botija, C., Dandurand, J., Benitez-Amaro, A., Nasarre, L., ... Llorente-Cortés, V. (2017). Conformational and thermal characterization of left ventricle remodeling post-myocardial infarction. *Biochimica et Biophysica Acta*, *1863*, 1500–1509. https://doi.org/10.1016/j.bbadis.2017.02.025

Sanada, S., Komuro, I., & Kitakaze, M. (2011). Pathophysiology of myocardial reperfusion injury: Preconditioning, postconditioning, and translational aspects of protective measures. *American Journal of Physiology. Heart and Circulatory Physiology*, *301*, H1723–H1741. https://doi.org/10.1152/ajpheart.00553.2011

Singh, M., Shah, T., Khosla, K., Singh, P., Molnar, J., Khosla, S., & Arora, R. (2012). Safety and efficacy of intracoronary adenosine administration in patients with acute myocardial infarction undergoing primary percutaneous coronary intervention: A meta-analysis of randomized controlled trials. *Therapeutic Advances in Cardiovascular Disease*, *6*, 101–114. https://doi.org/10.1177/1753944712446670

Urmaliya, V. B., Pouton, C. W., Ledent, C., Short, J. L., & White, P. J. (2010). Cooperative cardioprotection through adenosine A1 and A2A receptor agonism in ischemia reperfused isolated mouse heart. *Journal of Cardiovascular Pharmacology*, *56*, 379–388. https://doi.org/10.1097/FJC.0b013e3181f03d05

Xi, J., McIntosh, R., Shen, X., Lee, S. R., Chanoit, G., Criswell, H., ... Xu, Z. (2009). Adenosine A2A and A2B receptors work in concert to induce a strong protection against reperfusion injury in rat hearts. *Journal of Molecular and Cellular Cardiology*, *47*, 684–690. https://doi.org/10.1016/j.yjmcc.2009.08.009

Xi, L., Das, A., Zhao, Z. Q., Merino, V. F., Bader, M., & Kukreja, R. C. (2008). Loss of myocardial ischemic postconditioning in adenosine A1 and bradykinin B2 receptors gene knockout mice. *Circulation*, *118*, S32–S37. https://doi.org/10.1161/CIRCULATIONAHA.107.752865

Yang, T. T., Weng, S. F., Zheng, N., Pan, Q. H., Cao, H. L., Liu, L., ... Mu, D. W. (2011). Histopathology mapping of biochemical changes in myocardial infarction by fourier transform infrared spectral imaging. *Forensic Science International*, *207*, 34–39. https://doi.org/10.1016/j.forsciint.2010.12.005

Ye, X., & Yang, D. (2009). Recent advances in biological strategies for targeted drug delivery. *Cardiovascular & Hematological Disorders Drug Targets*, *9*, 206–221. https://doi.org/10.2174/187152909789007025

Yellon, D. M., & Hausenloy, D. J. (2007). Myocardial reperfusion injury. *The New England Journal of Medicine*, *357*, 1121–1135. https://doi.org/10.1056/NEJMra071667

Zhan, E., McIntosh, V. J., & Lasley, R. D. (2011). Adenosine A2A and A2B receptors are both required for adenosin A receptor-mediated cardioprotection. *American Journal of Physiology. Heart and Circulatory Physiology*, *301*, H1183–H1189. https://doi.org/10.1152/ajpheart.00264.2011

Zhao, Z. Q. (2010). Postconditioning in reperfusion injury: A status report. *Cardiovascular Drugs and Therapy*, *24*, 265–279. https://doi.org/10.1007/s10557-010-6240-1

Zong, X., Bien, H., Chung, C., Yin, L., Fang, D., Hsiao, B., ... Entcheva, E. (2005). Electrospun fine-textured scaffolds for heart tissue constructs. *Biomaterials*, *26*, 5330–5338. https://doi.org/10.1016/j.biomaterials.2005.01.052

SUPPORTING INFORMATION

Additional supporting information may be found online in the Supporting Information section at the end of the article.

Figure S1. a) Optical image of ADMMP after release at 24 h; b) chemical surface map; c) spectra of different surface areas.

Figure S2. SEM image of surface of patch detached from 3_AMI + ADMMP tissue after 24 h of follow- up (a); FT-IR analysis carried out directly on the 3_AMI + ADMMP tissue at the interface with the patch: chemical surface map (b); spectra of different surface areas (c).

Figure S3. FT-IR Chemical Imaging carried out on the 4_AMI + ADMMP tissue that was at contact with the device after 3 months: a) Chemical map of the myocardial tissue; b) Spectrum acquired in the tissue area.

Figure S4. FT-IR Chemical Imaging a) spectra acquired at three different points of the area at the interface with ADMMP, b) spectra acquired in the region 1800–1500 cm^{-1} in myocardial samples of 2_AMI + MMP at level of proximal, distal and control areas.